JOURNAL OF CATALYSIS 91, 338–351 (1985)

Carbon-Supported Fe–Ru Catalysts Prepared from Stoichiometric Mixed-Metal Carbonyl Clusters

MARK KAMINSKY,* KI J. YOON,† GREGORY L. GEOFFROY,* AND M. ALBERT VANNICE†,[1]

*Departments of Chemistry and †Chemical Engineering, The Pennsylvania State University, University Park, Pennsylvania 16802

Received May 14, 1984; revised August 29, 1984

Highly dispersed Fe–Ru bimetallic crystallites were obtained on an amorphous carbon black using mixed-metal carbonyl precursors. These catalysts were characterized by chemisorption of CO and H_2 at 195 and 300 K and their kinetic properties in the CO hydrogenation reaction were determined. If not exposed to air, only a low-temperature pretreatment at 473 K was required to reduce essentially all the Fe in the $Fe_3(CO)_{12}$ catalyst to activate it. In contrast, air exposure did not affect the reduction behavior of the Ru-containing catalysts. Both chemisorption and kinetic behavior indicated that surface enrichment in Fe occurred in these small crystallites after reduction, which is consistent with studies of bulk Fe–Ru systems. Turnover frequencies (TOF) for CH_4 and total hydrocarbon formation increased in parallel with the increase in surface Ru concentration whereas the TOF for CO_2 smoothly decreased. Distinct differences in catalytic behavior were observed for a coimpregnated $Fe_3(CO)_{12}$ plus $Ru_3(CO)_{12}$ catalyst, compared to the mixed-metal cluster catalysts, indicating a lack of homogeneity when using this procedure. Scanning transmission electron microscope micrographs showed a raft-like structure for the metal crystallites in the small-pore structure of the carbon, and this morphology may be partially responsible for the differences in catalytic behavior and the activity stability which exists between these carbon-supported metals and the same metals on other supports.

INTRODUCTION

Lack of control of product selectivity has been the principal problem associated with the Fischer–Tropsch synthesis reaction. Supported alloy catalysts offer one method to alter product selectivities, especially regarding olefin/paraffin ratios and oxygenate formation, compared to single-component systems since electronic and crystal structure effects can change the relative rates of parallel reactions and perhaps suppress undesirable ones. Vannice and Garten (*1*) demonstrated such effects in a supported Fe–Pt catalyst where a change in the synthesis rate on the Fe sites was attributed to electron withdrawal from the iron by the platinum. Supported bimetallic systems of Fe and Ru have been shown to possess unique catalytic properties which also could arise from changes in the electronic nature of the catalyst (*2–4*).

One promising method of obtaining such supported bimetallic catalysts is by utilizing organometallic mixed-metal carbonyl clusters as the metal precursor (*5–10*). Several advantages exist from such an approach. A variety of stoichiometric metal compositions can be obtained; for example, in going from $H_2FeRu_3(CO)_{13}$ to $Fe_2Ru(CO)_{12}$ the Fe/Ru ratio changes from 0.33 to 2. Such initially uniform metal compositions would be difficult to guarantee by coimpregnation techniques. Another advantage is that the mixed-metal carbonyl cluster should be able to be activated just by heating to a temperature that would decompose the cluster to yield reduced metal and CO, assuming the metal does not interact with the support. This decomposition temperature is usually below 475 K, and therefore it should be possible to obtain reduced metal

[1] To whom inquiries should be sent.

0021-9517/85 $3.00

at much less severe reduction conditions than those used for conventional metal salt precursors. This has the advantage of reducing the possibility of sintering and crystallite growth.

The use of high-surface-area carbon as a support has been found to stabilize highly dispersed iron particles formed from an aqueous impregnation technique using $Fe(NO_3)_3$ (*11*), and it was of interest to determine if metal carbonyl precursors would also produce well-dispersed metal crystallites. In addition, earlier studies indicated that using carbon as a support can also alter catalytic behavior of metals such as iron and ruthenium (*11–13*). Finally, the use of carbon to provide an inert, noninteracting surface could alleviate the difficulty often encountered on other supports in reducing all the metal, especially iron. On a support like Al_2O_3, iron cations strongly interact with the support surface which frequently results in a large fraction of iron that cannot be reduced to the zero-valent state. Herein we describe the genesis, characterization, and catalytic behavior of a series of such carbon-supported Fe, Ru, and Fe/Ru catalysts prepared from stoichiometric metal carbonyl precursors.

EXPERIMENTAL

The amorphous carbon support used for these studies was Cabot Corporation's CSX-203. As received, this carbon contained 0.59% sulfur, as determined by Leco titration. Catalysts prepared using the as-received CSX-203 carbon exhibited no CO hydrogenation activity, so the carbon samples were treated at 1223 K for 12 h under flowing H_2 to decrease the sulfur content (*11*). This desulfurized CSX-203 had a N_2 BET surface area of 1410 m^2/g and contained 0.13% sulfur (Table 1). Before supporting the metal clusters, the carbon was heated to 573 K under vacuum (10^{-4} kPa) for 8 h in order to remove physisorbed water.

The clusters $Fe_3(CO)_{12}$ (*14*), $Ru_3(CO)_{12}$ (*15*), $FeRu_2(CO)_{12}$ (*16*), $H_2FeRu_3(CO)_{13}$ (*17*), and $Fe_2Ru(CO)_{12}$ (*16*) were prepared following known methods of synthesis. They were dispersed on the carbon by incipient wetness impregnation using dry and degassed THF as solvent. The coimpregnated $Fe_3(CO)_{12}$ + $Ru_3(CO)_{12}$ sample was prepared by sequential impregnation of the two clusters. The entire impregnation was done under anaerobic conditions using standard Schlenk techniques (*18*). The preparation of the $Fe(NO_3)_3$ sample has been described previously (*11*). Samples were dried by evacuating to 10^{-4} kPa for 8 h at room temperature. The catalysts were exposed to air for approximately 15 min when the chemisorption and microreactor cells were loaded; however, one sample of $Fe_3(CO)_{12}$/carbon was also loaded without air exposure and nearly identical behavior was obtained after reduction at 673 K.

TABLE 1

Impurities in Desulfurized Carbon CSX-203 as Determined by Plasma Emission Spectrometry

Element	Amount (ppm)	Element	Amount (ppm)
Si	>6	Ca	1,730
Al	2	Na	3
Tl	2	K	3
Fe	22	S (as SO_3)	1,340
Mg	2		

All catalyst samples were subjected to two different pretreatments prior to adsorption or kinetic studies. The low-temperature reduction pretreatment (LTR) consisted of heating to 473 K under flowing hydrogen (20 cm^3/min) and reducing at this temperature for 2–5 h until no solvent in the gas stream could be detected by gas chromatography. The high-temperature reduction pretreatment (HTR) consisted of heating to 673 K under flowing hydrogen (20 cm^3/min) and reducing at this temperature for 16 h.

For H_2 and CO uptake measurements, the samples were evacuated and then heated to 673 K for 30 min before cooling under dynamic vacuum to 300 K for H_2 and

300 or 195 K for CO chemisorption. The zero-pressure intercept of the linear, high-pressure portion of the H_2 isotherm was chosen to represent monolayer hydrogen coverage, and for CO the dual isotherm method was used with the difference at 200 Torr (26.7 kPa) representing irreversible CO adsorption. For kinetic studies, the samples were cooled under flowing H_2 to the desired temperature.

The experimental apparatus and procedure have been described elsewhere (*19, 20*). The hydrogen uptake measurements were done at room temperature and the CO uptake measurements were carried out at room temperature and 195 K. The apparatus was a mercury-free, glass adsorption system capable of achieving a dynamic vacuum of 1×10^{-6} Torr. Gas pressures were measured using a Texas Instruments precision pressure gauge. During hydrogen adsorption measurements at room temperature and the CO adsorption measurements at 195 K, no slow adsorption was observed; hence the first data point was taken after 15–30 min of exposure to the adsorbate gas and each remaining data point was taken 5 min after each pressure increment. During the CO adsorption measurements at room temperature, however, a slow continuous pressure decrease was observed for all the catalysts, and the first data point was taken after 1 h of exposure and each remaining data point was taken 10 min after each pressure increase.

The kinetic data were obtained under differential reaction conditions using a glass, plug-flow microreactor operating at a total pressure of 103 kPa (1 atm) (*19, 20*). Product analyses were obtained using a Perkin–Elmer Sigma 3 gas chromatograph fitted with Chromosorb 102 columns and subambient temperature programming. A Perkin–Elmer Sigma 1 integrator was interfaced to this system. Catalyst charges to the reactor were 0.2–0.5 g and CO conversions near 7% or lower were maintained so that the reactor operated in a differential mode. Each set of kinetic data was obtained after 20 min onstream following a 20-min exposure to pure H_2. Helium was used as a diluent when the partial pressure of H_2 or CO was varied. The purities of gases used were H_2 (99.999%, M. G. Scientific), CO (Matheson Purity, 99.999%), and He (99.999%, M. G. Scientific). All gases were further purified by passing through molecular sieves, Drierite, and Oxytraps as appropriate. Metal loadings were determined by neutron activation analyses using Fe and Ru standards of known concentration for calibration, and the results are given in Table 2.

TABLE 2

Percentage Metal Loadings on CSX-203-Supported Catalysts

Metal precursor	Fe (wt%)	Ru (wt%)	Fe/Ru mole ratio	μmole total metal/g catalyst
$Fe(NO_3)_3$	5.0	—	—	893
$Fe_3(CO)_{12}$	4.4	—	—	786
$Fe_3(CO)_{12} + Ru_3(CO)_{12}$	4.2	2.0	3.76	943
$Fe_2Ru(CO)_{12}$	0.97	0.77	2.27	248
$FeRu_2(CO)_{12}$	0.70	2.35	0.536	358
$FeRu_3H_2(CO)_{13}$	0.47	2.6	0.32	343
$Ru_3(CO)_{12}$	—	6.3	0	624

For STEM analysis, the catalyst particles were ground in air by pressing 4–6 mg between two glass slides. The ground catalyst was dispersed in 10 ml of toluene using ultrasound for 45 min. One minute after the ultrasound was turned off, a drop was taken from the middle of the suspension and applied to a carbon film, 10–20 nm thick, that was supported by a 400-mesh copper grid. Specimens were examined at 120 kV using a Phillips EM-420 STEM system.

RESULTS

Chemisorption

The catalysts studied, their percentage metal loadings, and the total metal loading in moles of metal per gram of catalyst are listed in Table 2. For brevity, the remainder of the tables do not include the percentage metal loadings. Before discussing our CO and H_2 chemisorption results, it is appropriate to briefly review what is known about

chemisorption of these gases on Fe and Ru metals. In the following discussion H_a and CO_a refer to adsorbed hydrogen and CO, M_s refers to a surface metal atom, and M_t represents the total number of metal atoms.

Hydrogen is known to not chemisorb to any significant extent on small Fe crystallites (*20–22*). However, for Ru a hydrogen adsorption stoichiometry giving H_a/Ru_s values near unity at 300 K has been found by Dalla Betta to give good agreement between particle sizes calculated by hydrogen chemisorption and by electron microscopy (*23*).

Although standard CO chemisorption techniques do not exist for iron, good agreement among different techniques to measure particle size has been obtained by assuming the presence of bridge-bonded CO at 195 K, $CO_a/Fe_s = 0.5$ (*20, 24*). Carbon monoxide uptake on well-dispersed iron at 300 K is known to exceed that at 195 K by a factor of 3 or higher (*20*). These high CO_a/Fe_s ratios which exceed unity at 300 K imply subcarbonyl formation which has been attributed to the presence of small Fe crystallites (*20*). Such subcarbonyl species have been previously reported for highly dispersed Ru (*25, 26*), Rh (*27*), and Ni (*28*). Carbon monoxide chemisorption on Ru is more ambiguous than CO chemisorption on Fe since formation of several subcarbonyls has been reported for highly dispersed ruthenium catalysts using infrared spectroscopic methods (*25, 29, 30*). Such subcarbonyl formation would lead to the CO_a/H_a or CO_a/Ru_s ratios higher than unity which have been reported (*25, 29, 31*).

The CO and hydrogen uptakes on the freshly reduced catalysts using pretreatments LTR and HTR are listed in Table 3. For the Fe-only catalysts ($Fe(NO_3)_3$ and $Fe_3(CO)_{12}$) the hydrogen uptakes were negligible. For CO chemisorption, if we assume that the 195 K data give the accepted ratio of 0.5 for CO_a/Fe_s, then the 300 K data imply corresponding ratios of 3.9 and 1.1 for $Fe(NO_3)_3$ and $Fe_3(CO)_{12}$, respectively. Since the Fe–Ru catalysts were made from metal carbonyls, the results for $Fe_3(CO)_{12}$ were used in all further comparisons between the Fe and Fe/Ru samples.

For the Ru-only catalyst using $Ru_3(CO)_{12}$, the amount of CO chemisorbed at 300 K is 1.2–1.3 times higher than that at 195 K, which implies some subcarbonyl formation at the higher temperature (*25, 29, 31*), if a CO_a/Ru_s ratio of unity is assumed at 195 K. The CO(195 K)/H_a ratios are close to unity, showing consistency between the assumptions made.

For the Fe–Ru bimetallic catalysts the

TABLE 3

Chemisorption on Fresh, Reduced CSX-203-Supported Fe, FeRu, and Ru Catalysts

Metal complex	Pretreatment	H_2 (μmole/g cat.)	CO (195 K) (μmole/g cat.)	CO (300 K) (μmole/g cat.)	Uptake ratios			
					H/M_t	CO/M_t (300 K)	CO/M_t (195 K)	CO (300 K) / CO (195 K)
$Fe(NO_3)_3$	HTR	—	60	470	—	0.526	0.067	7.85
$Fe_3(CO)_{12}$	LTR	—	46	—	—	—	0.059	—
	HTR	1.0	145	315	0.002	0.40	0.185	2.2
$Fe_3(CO)_{12}$ +	LTR	17.0	245	—	0.036	—	0.260	—
$Ru_3(CO)_{12}$	HTR	19.0	200	297	0.040	0.32	0.212	1.5
$Fe_2Ru(CO)_{12}$	LTR	7.6	140	255	0.062	1.03	0.565	1.8
	HTR	8.8	100	175	0.071	0.71	0.403	1.8
$FeRu_2(CO)_{12}$	LTR	26.0	200	307	0.145	0.86	0.559	1.5
	HTR	27.5	133	212	0.154	0.59	0.372	1.6
$H_2FeRu_3(CO)_{13}$	LTR	40.0	220	—	0.233	—	0.641	—
	HTR	27.5	230	334	0.160	0.97	0.671	1.4
$Ru_3(CO)_{12}$	LTR	149.0	250	322	0.478	0.52	0.401	1.3
	HTR	115.0	260	308	0.369	0.49	0.417	1.2

TABLE 4

Catalytic Activity for CO Hydrogenation for CSX-203-Supported Metals

Metal complex	Pretreatment	Activity		Activity {mole · s^{-1} (mole M_t metal)$^{-1}$} × 1000[a]			
		$\frac{\mu mole\ CO}{s \cdot g\ cat.}$	$\frac{\mu mole\ CH_4}{s \cdot g\ cat.}$	CO to hydrocarbons	CH_4	CO_2	% Conversion of CO to hydrocarbons
$Fe(NO_3)_3$	HTR	0.30	0.123	0.34	0.138	0.153	3.1
$Fe_3(CO)_{12}$	LTR	0.0035	0.0035	0.0045	0.0045	0.0056	0.04
	HTR	1.13	0.338	1.44	0.430	0.770	6.0
$Fe_3(CO)_{12}$ +	LTR	1.64	0.466	1.74	0.494	1.591	7.8
$Ru_3(CO)_{12}$	HTR	1.26	0.300	1.34	0.318	1.43	6.0
$Fe_2Ru(CO)_{12}$	LTR	0.624	0.451	2.52	1.82	1.23	2.9
	HTR	0.692	0.387	2.79	1.56	1.20	3.2
$FeRu_2(CO)_{12}$	LTR	2.35	1.73	6.56	4.83	0.822	5.8
	HTR	1.80	1.33	5.03	3.72	0.623	4.4
$H_2FeRu_3(CO)_{13}$	LTR	2.18	2.04	6.36	5.95	0.903	5.2
	HTR	1.89	1.63	5.51	4.75	0.496	4.9
$Ru_3(CO)_{12}$	LTR	2.49	2.47	4.00	3.96	0.192	6.5
	HTR	2.26	2.21	3.62	3.54	0.160	5.9

[a] P = 101 kPa, H_2/CO = 3, T = 548 K.
[b] Based on M_s calculated from adsorbed CO, 195 K.

ratio of hydrogen atoms to total metal atoms increases steadily as the Ru content increases, a trend which agrees with previous work (*2, 4*) and is expected since Ru chemisorbs H_2 whereas small Fe crystallites do not. Similarly, the gradual decrease in the ratio of CO adsorbed at 300 K to that adsorbed at 195 K with increasing Ru content is consistent with the CO stoichiometries discussed above.

The bimetallic catalysts show characteristics with regard to reduction temperature that is indicative of contact between the Fe and Ru atoms. For the Ru-only and the Fe–Ru catalysts, a temperature of 473 K appears high enough to obtain reduced metal. The Fe-only catalysts were not completely reduced at 473 K, as evidenced by the lack of CO uptake after an LTR pretreatment compared to an HTR pretreatment. The presence of Ru thus facilitates the reduction of Fe. The $Fe_3(CO)_{12}$ and $Ru_3(CO)_{12}$ coimpregnated sample showed the same behavior as the bimetallic clusters in terms of reduction temperature, again implying intimate contact in this sample.

Kinetic Studies

For the $Fe_3(CO)_{12}$/CSX-203 catalyst the activity after pretreatment LTR was much lower than that after pretreatment HTR, as shown in Table 4, due to incomplete reduction of Fe under low-temperature conditions. To test the effect of air exposure on activities, one sample was evaluated that had never been exposed to air. This showed similar activities after the two pretreatments which were also similar to that after pretreatment HTR for the $Fe_3(CO)_{12}$ catalyst that was exposed briefly to air, indicating that exposure to air increases the difficulty of reduction of this catalyst.

For ruthenium-containing catalysts, the activity per gram catalyst after pretreatment HTR was nearly equal to or lower than that after pretreatment LTR, consistent with the chemisorption results which showed a decrease in CO uptakes following

TABLE 5

Product Selectivity[a]

Catalyst	% CO to hydrocarbon conversion	$\frac{Fe_t}{Ru_t}$	Hydrocarbons (mole%)							C_2–C_3 Olefin/paraffin ratio
			C_1	C_{2-}	C_2	C_{3-}	C_3	C_4	C_{5+}	
$Fe(NO_3)_3$	3.1	—	61	3	27	—	7	1	1	0.09
$Fe_3(CO)_{12}$	6.0	—	56	5	19	3	4	7	5	0.36
$Fe_3(CO)_{12}$ + $Ru_3(CO)_{12}$	6.0	3.76	50	10	9	16	—	7	7	2.9
$Fe_2Ru(CO)_{12}$	3.2	2.27	76	3	16	—	—	3	1	0.19
$FeRu_2(CO)_{12}$	4.4	0.55	88	1	8	—	2	1	1	0.08
$H_2FeRu_3(CO)_{13}$	4.9	0.32	95	—	4	—	0.6	0.6	0.3	—
$Ru_3(CO)_{12}$	5.9	—	99	—	1	—	—	—	—	—

[a] Measured after pretreatment HTR; T = 548 K, P_T = 100 kPa, H_2/CO = 3.

pretreatment HTR, relative to LTR, as shown in Table 3. Again, it indicates the ease of reduction when Ru is present, and either pretreatment provides similar turnover frequency (TOF) values for the Ru-containing catalysts. Even though the chemisorption capacity decreased after pretreatment HTR, presumably due to crystallite growth, the selectivity was independent of the pretreatment. Selectivities to hydrocarbon products measured after pretreatment HTR at 548 K, P = 100 kPa, and H_2/CO = 3 are listed in Table 5. The specific activities in Table 6 were calculated based on M_s values assuming CO(195 K)/Ru_s = 1 for the Ru-only catalyst and CO(195 K)/Fe_s = 1/2 for the Fe-only catalyst. For the Fe–Ru bimetallic catalysts, there is some uncertainty regarding surface stoichiometries, and a CO(300 K)/M_s ratio

TABLE 6

Specific Activity of Cluster Catalysts in TOF (molec. s^{-1} M_s^{-1}) × 10^3[a]

	Pretreatment	N_{CO}		N_{CH_4}		N_{CO_2}[b]
		[b]	[c]	[b]	[c]	
$Fe(NO_3)_3$	HTR	2.5	—	1.03	0.26	1.18
$Fe_3(CO)_{12}$	LTR	0.012	—	0.012	—	0.15
	HTR	3.9	—	1.2	1.07	2.08
$Fe_3(CO)_{12}$ +	LTR	4.5	—	1.3	—	4.2
$Ru_3(CO)_{12}$	HTR	3.4	4.24	0.83	1.0	3.76
$Fe_2Ru(CO)_{12}$	LTR	3.4	2.45	2.5	1.77	1.68
	HTR	3.8	4.0	2.1	2.2	1.6
$FeRu_2(CO)_{12}$	LTR	13.0	7.65	9.6	5.64	1.64
	HTR	10.0	8.5	7.4	6.3	1.22
$H_2FeRu_3(CO)_{13}$	LTR	9.5	—	8.9	—	1.14
	HTR	8.2	5.7	7.1	4.9	0.65
$Ru_3(CO)_{12}$	LTR	9.6	7.7	9.5	7.7	0.46
	HTR	8.7	7.3	8.5	7.2	0.38

[a] T = 548 K, P_T = 100 kPa, H_2/CO = 3.

[b] Based on calculated M_s values after HTR (see Table 9).

[c] Based on CO uptake at 300 K after corresponding LTR or HTR pretreatment. N_{CO} = CO molec. converted to hydrocarbons (no CO_2).

TABLE 7

Activation Energies and Reaction Orders

	E_a (kJ mole^{-1})		$r = kP(H_2)^xP(CO)^y$					
	CO to hydrocarbons	CH_4	CO to hydrocarbons		CH_4		CO_2	
			x	y	x	y	x	y
$Fe(NO_3)_3$	118	103	—	—	—	—	—	—
$Fe_3(CO)_{12}$	100	86	1.1	−0.53	1.0	−0.67	0.0	0.0
$Fe_3(CO)_{12}$ + $Ru_3(CO)_{12}$	97	81	0.69	+0.12	0.96	−0.40	+0.21	—
$Fe_2Ru(CO)_{12}$	83	76	0.97	−0.46	1.0	−0.63	0.0	0.0
$FeRu_2(CO)_{12}$	92	87	0.91	−0.53	0.96	−0.56	0	−0.1
$H_2FeRu_3(CO)_{12}$	96	93	0.60	−0.61	0.63	−0.69	0	−0.4
$Ru_3(CO)_{12}$	90	90	0.59	−0.37	0.59	−0.37	0	0.25

of 1/1 was used to calculate a minimum TOF while M_s values based on surface compositions calculated from the chemisorption behavior were used to calculate a more realistic TOF. The activation energies shown in Table 7 were calculated using activities in the temperature range of 473 to 593 K, and the reaction orders, also shown in Table 7, were determined at a constant temperature of 548 K.

There is evidence that surface segregation of Fe may have occurred in these catalysts. The heat treatment was varied for the $H_2FeRu_3(CO)_{13}$ catalyst, and Table 8 shows the hydrogen uptake decreased with the length of pretreatment time, whereas the CO uptake stayed the same. This would indicate segregation of Fe to the surface of the FeRu crystallites, a conclusion which is supported by the surface composition calculations based on the chemisorption data in Table 3, which will be discussed later.

TABLE 8

Chemisorption of H_2 and CO as a Function of Reduction Time for $H_2FeRu_3(CO)_{13}$ on CSX-203 (μmole/g cat.)

Pretreatment	H_2 at RT	CO (195 K)
2 h, 200°C, 20 sccm H_2	40.00	220.0
16 h, 400°C, 20 sccm H_2	27.50	230.0
32 h, 400°C, 20 sccm H_2	13.24	217.0

In order to get additional information about particle sizes, high-resolution STEM photographs were taken of the $FeRu_2(CO)_{12}$/CSX-203 catalyst after it had been reduced by an HTR pretreatment. Figure 1 is a representative photograph of this catalyst at a magnification of approximately 2.2×10^6, at which a resolution of 2 Å is achieved. Several metal particles can be seen varying in size from about 20 to 60 Å with fringe spacings varying from 4.4 Å (B) to 9.2 Å (A). The particles seem to be extremely thin since the support can clearly be seen through the lattice fringes.

DISCUSSION

Estimation of Surface Composition of Fe–Ru Clusters on Carbon

Characterization of such small bimetallic clusters such as those discussed herein is quite difficult; however, the composition of the metal surface layer in atom fraction of iron, Fe_s/M_s, was estimated after HTR using the previously discussed assumptions of CO and H_2 adsorption stoichiometries on Fe and Ru. Greater confidence was placed in the CO stoichiometries at 195 K com-

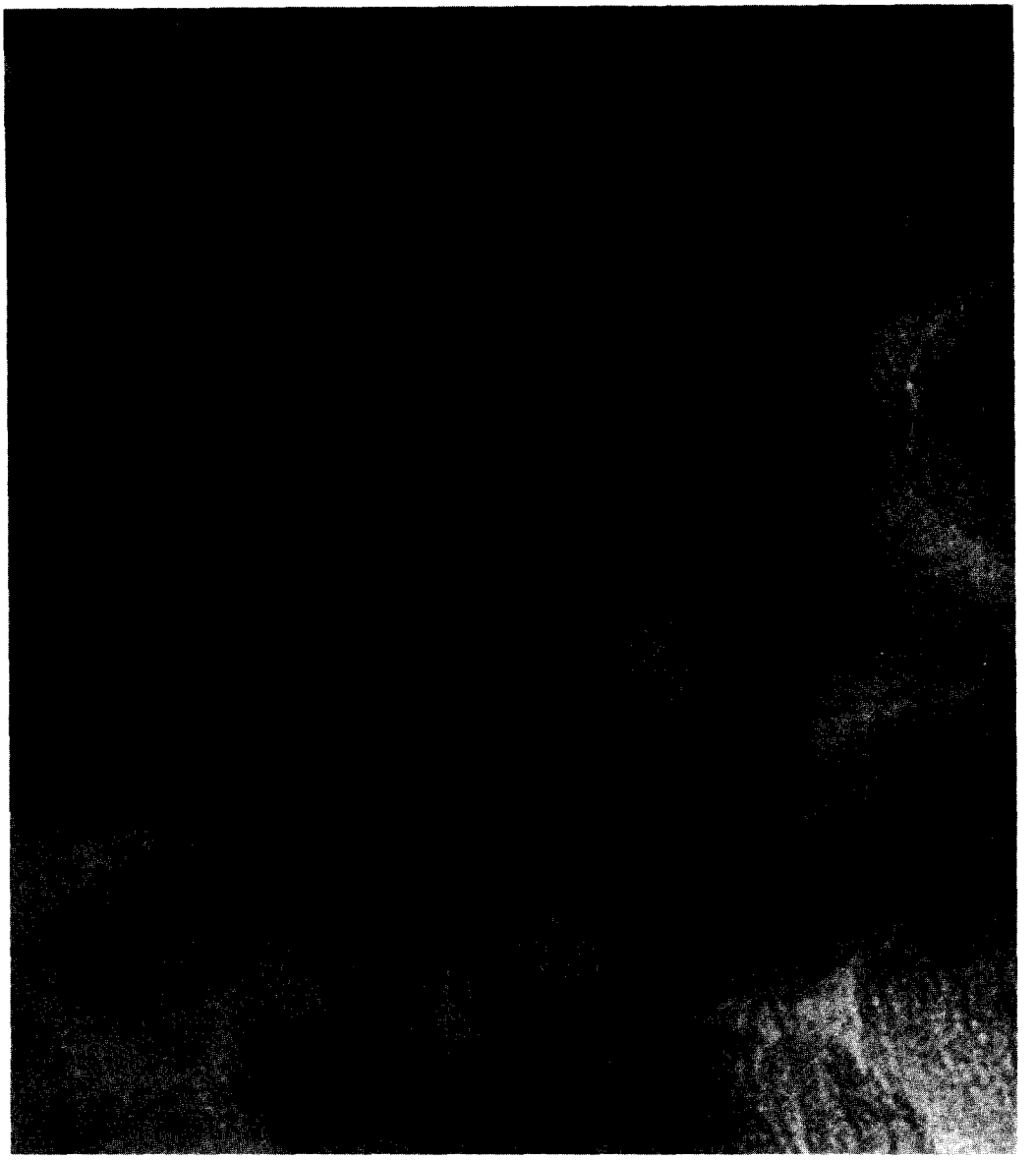

FIG. 1. STEM photomicrograph of $FeRu_2(CO)_{12}$/CSX-203 catalyst after kinetic analysis. Magnification is ~2,200,000. Raft-like structure is indicated by metal particles A and B.

pared to those at 300 K because the former are less ambiguous and there is less chance of subcarbonyl formation or dissociation of CO on Ru. An obvious limitation is that the Fe_s and Ru_s values cannot exceed the total Fe and total Ru values based on the metals analyses listed in Table 2. Based on the assumptions that the adsorption stoichiometries were $H_a/Ru_s = 1$ at 300 K, $CO_a/Ru_s = 1$ at 195 K, $CO_a/Fe_s = 0.5$ at 195 K on Fe-rich surfaces and CO_a/Fe_s at 195 K = 1 on Ru-rich surfaces because of the sharp decrease in Fe–Fe nearest neighbors, the surface compositions in Table 9 were calculated using the chemisorption data in Table 3. The procedure was as follows. The H_2

TABLE 9

Estimation of Surface Composition after HTR

Metal precursor	Fe_t/M_t	Fe_s/M_s	M_s/M_t	Ru_s/M_t	Fe_s/M_t	Predicted CO_a/M_t ratio at 300 K[a]	Actual CO/M_t at 300 K
$Fe(NO_3)_3$	1.0	1.0	0.13 (5.8)[b]	—	0.13	—	—
$Fe_3(CO)_{12}$	1.0	1.0	0.37 (2.0)[b]	—	0.37	—	—
$Fe_3(CO)_{12}$ + $Ru_3(CO)_{12}$	0.79	0.89	0.38	0.040	0.344	0.38	0.32
$Fe_2Ru(CO)_{12}$	0.69	0.90	0.73	0.073	0.661	0.73	0.71
$FeRu_2(CO)_{12}$	0.35	0.69	0.50	0.153	0.349	0.50	0.59
$H_2FeRu_3(CO)_{13}$	0.24	0.37	0.67	0.420	0.250	0.75[c]	0.97
$Ru_3(CO)_{12}$	0.0	0	0.42	0.417	0	—	

[a] Assuming $CO_a/Fe_s = CO_a/Ru_s = 1$.
[b] Average crystallite size (nm).
[c] Assuming CO/Ru = 1.2.

uptake was used to define the number of Ru_s atoms. The appropriate number of Fe_s atoms was then chosen to give the measured CO uptake at 195 K. A CO/Fe_s stoichiometry of 0.5 was used for all samples except the $FeRu_3$ catalyst, which was the only one indicating an Ru-rich surface. This catalyst also had an anomalously low H_2 uptake and the H/Ru_s stoichiometry had to be relaxed in order to predict sufficient CO uptake at 195 K because the total amount of Fe in the sample was only 86 μmole Fe/g cat. The estimated H_a/Ru_s value for this $ReFu_3$ sample was 0.4. As a sample calculation, the Fe_2Ru/carbon catalyst adsorbed 18 μmole H atoms/g and therefore defined a Ru_s value of this amount. The number of Fe_s atoms required to predict a CO uptake of 100 μmole/g was 164 μmole Fe_s/g. The surface composition was therefore Ru_s/M_s = 18/182 = 0.10 and the dispersion M_s/M_t was 182/248 = 0.73.

Assuming a CO_a/M_s ratio of unity, CO uptakes predicted at 300 K are listed in Table 9. The actual values are similar for the coimpregnated and the Fe_2Ru samples whereas a limited amount of subcarbonyl formation appears to occur on the $FeRu_2$ and $FeRu_3$ samples. Regardless, actual uptakes are quite reasonable based on the number of surface metal atoms determined.

It should be mentioned that an alternative method to determine surface composition was used based on a different set of assumptions, i.e., using CO_a/Ru_s = 1 at 195 K, CO_a/Ru_s = 1.2 at 300 K (from Table 3), CO_a/Fe_s = 0.5 at 195 K and CO_a/Fe_s = 1 at 300 K. These calculations resulted in the same conclusion that the surface was Fe-rich; however, the curves in Fig. 2 were not as smooth and, more importantly, H_a/Ru_s ratios were always much less than unity, ranging from 0.3 to 0.8. Consequently, we prefer the former approach.

The major conclusion that can be drawn from the surface compositions in Table 9 is that *the surfaces of the metal crystallites are enriched in Fe as compared to the bulk composition,* and this is illustrated by the data plotted in Fig. 2. Equal bulk and surface compositions would give a 45° line; however, the fact that all values lie below this line indicates that the surface is enriched in Fe. It should be mentioned that the bulk phase diagram for the Fe–Ru system shows that complete miscibility and a single phase occur for these metals for all compositions used in these studies (above 24% Ru) (*32*). This is consistent with data reported by Ott *et al.* (*33, 34*) who found that for unsupported Fe–Ru alloys the surface was primarily composed of Fe even

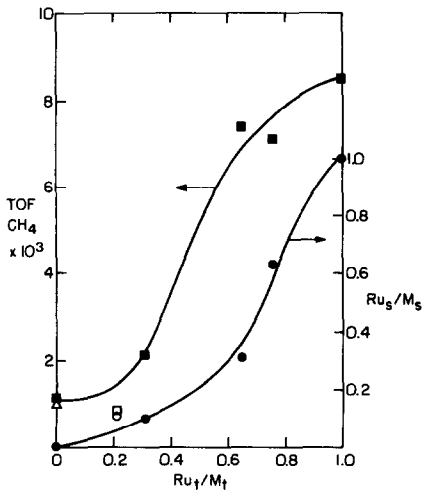

FIG. 2. Dependence of surface compositions (●), and TOF for CH_4 (■), on overall metal composition, Ru_t/M_t. The coimpregnated $Fe_3(CO)_{12}$ + $Ru_3(CO)_{12}$ sample is indicated by the open symbols, and the Fe-only sample prepared from $Fe(NO)_3$ is indicated by a triangle.

when the percentage of Ru in the bulk was above 25 at.%. This was expected from the fact that Fe has a lower surface energy than Ru. For example, the bond enthalpy parameters for Fe(bcc) and Ru(hcp) are 24.17 and 26.67 kcal/mole, respectively (*33*). Further, the data in Table 8 show that prolonged heating induces further surface enrichment in Fe, since the amount of H_2 chemisorbed decreases with time, at least for the $H_2FeRu_3(CO)_{13}$/CSX-203 sample.

Particle Size Considerations

The dispersions are relatively high for all the metal carbonyl catalysts and range from 0.4 to 0.8. Particle size estimations from chemisorption data for Fe and Ru catalysts have previously assumed particles to be spherical or cube-shaped (*11, 19, 23*). As one can see from Fig. 1, the metal particle shape on this amorphous carbon is almost two-dimensional so the previously reported estimations of particle size using spheres or cube-shaped models may not apply to this system. Such behavior has not been previously reported for carbon-supported metal catalysts. However, this result is still consistent with the high dispersions found by chemisorption since a two-dimensional particle would have a high M_s/M_t ratio regardless of the diameter.

Different lattice fringe spacings in the various particles in Fig. 1 are apparent but they are not an unambiguous indication of a difference in metal composition. Other factors such as differences in the thickness of the metal particle can also shift the fringe spacings (*35*). An effect from the support, such as epitaxy or pseudomorphism, could also change the lattice fringe spacings compared to bulk Fe and Ru spacings determined by X-ray crystallography. Regardless, the presence and stability of these raft-like crystallites on carbon are unexpected and surprising, and may indicate a more important role for the carbon support than previously assumed.

Catalytic Behavior

The much lower activity for the $Fe_3(CO)_{12}$ catalyst following a brief air exposure and an LTR pretreatment demonstrates the increased air sensitivities of supported metal carbonyl clusters compared to unsupported metal clusters. After an HTR pretreatment, the specific activity for CO hydrogenation of the Ru-only catalyst was 3–5 times higher than the Fe-only catalyst, and in terms of methanation activity the Ru-only catalyst was 7–10 times more active than the Fe-only catalyst. One obvious trend for the Fe–Ru bimetallic catalysts was the steady increase in CO hydrogenation and methanation specific activities with increasing Ru content. This increase paralleled the increase in the surface Ru concentration, as shown in Fig. 2. The specific activity for CO_2 formation steadily decreased with decreasing Fe content in the catalyst, with the exception of the $Fe_3(CO)_{12}$ plus $Ru_3(CO)_{12}$ catalyst which showed a relatively high activity for CO_2 formation. This trend in activities, shown in Fig. 3, is consistent with literature data (*33, 36–38*) which shows that Ru is a more active catalyst than Fe in terms of CO hy-

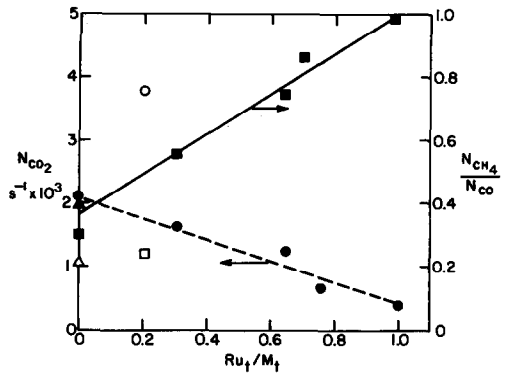

FIG. 3. Dependence of selectivity, N_{CH_4}/N_{CO} (■), and TOF for CO_2 (●), on overall metal composition, Ru_t/M_t. The coimpregnated $Fe_3(CO)_{12}$ + $Ru_3(CO)_{12}$ sample, is indicated by open symbols and the Fe-only sample prepared from $Fe(NO_3)_3$ is indicated by triangles. (▲) N_{CH_4}/N_{CO}, (△) N_{CO_2}.

drogenation but is less active than Fe in forming CO_2. The low specific activities for the Fe-only catalysts were similar to well-dispersed, carbon-supported Fe (*11, 19*) and SiO_2-supported Fe (*39*) previously reported in the literature. The differences in crystallite size, N_{CO} values, and olefin/paraffin ratios show that Fe/carbon catalysts prepared from Fe carbonyl precursors are not identical to those prepared from aqueous solutions of $Fe(NO_3)_3$, as indicated in Tables 5, 6, and 9.

The Ru-only catalyst had a TOF value one-half that reported previously for larger Ru crystallites (dispersion = 0.18) dispersed on Carbolac (*12*) and one-third that reported for well-dispersed Ru on Al_2O_3 (*40, 41*). Evidence exists that TOF values are lower on small Ru crystallites (*42*) and this could explain why the TOF on the present well-dispersed Ru cluster catalyst is an order of magnitude lower than TOF values observed on typical Ru catalysts (*12*). However, the low TOF values observed on both larger and smaller carbon-supported Ru particles indicates that the carbon itself may influence the specific activity. This may be a result of the raft-like particle formation which we have observed in our STEM studies.

The variation in TOF values as a function of bulk metal composition is shown in Fig. 2. This is consistent with our interpretation that surface enrichment in Fe occurs and surface Ru concentrations are especially low at lower bulk Ru compositions. This hypothesis is also supported by the low TOF values reported by Guczi *et al.* for coimpregnated, SiO_2-supported Fe and Ru carbonyl clusters containing 2.8 mole% Ru or less (*39*). Their reported TOF values were nearly the same as those obtained for their Fe/SiO_2 catalyst. Our catalyst prepared from $Fe_3(CO)_{12}$ plus $Ru_3(CO)_{12}$ seems to lie somewhat off all the curves provided by the Fe–Ru clusters and indicates some inhomogeneity among the metal crystallites. This variation between Fe–Ru catalysts with nearly identical metal loading and overall composition demonstrates the advantage of utilizing stoichiometric mixed-metal clusters to facilitate metal–metal contact and uniformity among the metal crystallites.

After an LTR pretreatment, the activities of the Fe–Ru catalysts were much higher than the LTR Fe carbonyl catalyst and were equal to or higher than activities of the same Fe–Ru catalysts after an HTR pretreatment. This behavior, coupled with the high CO adsorption values after an LTR step, provides strong evidence for Fe–Ru contact in which Ru catalyzes the reduction of the Fe component. This enhanced reducibility of Fe has been observed in other Fe–Group VIII metal bimetallic systems (*43*).

The product selectivities for the Fe-only catalysts listed in Table 5 are similar to those reported in the literature for other Fe/carbon catalysts (*11, 19*) except that the olefin/paraffin ratios for the catalysts in this study are lower than those found for other well-dispersed iron catalysts.

The Ru-only catalyst formed essentially only methane, and this selectivity to CH_4 is higher than reported for other Ru catalysts, except for one other previously reported Ru/carbon catalyst which gave close to 100% selectivity (*12*). Selectivities to CH_4 as low as 30 mole% have been reported at

these low pressures for unsupported Ru catalysts (*36, 37*). These low specific activities and very high selectivities to CH_4 over two different Ru/carbon catalysts with differing dispersions of 0.18 (*12*) vs 0.42 (this work) imply that the carbon support may have a more pronounced influence than crystallite size in catalytic behavior. Again this may be a consequence of the raft-like morphology of the metal particles that appears to occur in the small pores of high-surface-area amorphous carbons.

There was a gradual change in selectivity over the Fe–Ru catalysts when the Fe–Ru composition was varied, with the exception of the $Ru_3(CO)_{12}$ + $Fe_3(CO)_{12}$ catalyst. As the Ru content increased, the selectivity to methane increased almost linearly, as shown in Fig. 3, and the C_2–C_3 olefin/paraffin ratio decreased. However, the sequentially impregnated $Fe_3(CO)_{12}$ plus $Ru_3(CO)_{12}$/CSX-203 catalyst produced a higher olefin/paraffin ratio than any of the bimetallic Fe–Ru clusters. This is similar to the selectivity behavior of silica-supported Fe–Ru catalysts which were prepared by sequential impregnation of Ru and Fe salts (*2*). Therefore, varying the Fe–Ru precursor and the impregnation technique can affect the catalytic selectivity due probably to a variation in the contact between the two metal components because of the preparative technique. A more homogeneous system is expected with the bimetallic clusters.

The activation energies shown in Table 7 are within the ranges (71.0–117 kJ/mole) reported in the literature (*11, 38, 40, 41, 44, 45*), but no significant change was observed with varying metal composition. The reaction orders, also listed in Table 7, changed progressively with catalyst composition, except for the sequentially impregnated $Fe_3(CO)_{12}$ plus $Ru_3(CO)_{12}$/CSX-203 catalyst. The hydrogen reaction orders for the Fe-only catalyst were similar to literature values, ranging from 0.9 to 1.5 (*11*), but the CO reaction orders were significantly lower than previously reported results which were in the range of 0 to −0.26 (*11, 38*). This indicates that adsorbed CO or surface carbon inhibits CO hydrogenation even more than normal on these reduced-Fe clusters. For the Ru-only catalyst, the reaction order in hydrogen of 0.6 was also significantly lower than those reported in the literature for Ru, which varied between 1.1 and 2 (*38, 40, 41, 45*). The CO reaction orders were more consistent with the literature values which have ranged between 0 and −1.5. All the CO-to-total hydrocarbon reaction orders for the Fe–Ru bimetallic cluster catalysts fell between those for the pure-Fe and pure-Ru catalysts. As for the lower hydrogen reaction orders over the Ru-rich clusters, crystallite size, metal structure, or the support could affect this behavior and account for the low activities, but the predominant effect is not known at this time.

SUMMARY

This study has shown that well-dispersed, carbon-supported Fe–Ru bimetallic catalysts can be prepared from stoichiometric Fe–Ru mixed-metal carbonyl clusters. The presence of the Ru facilitates reduction of the iron and a low-temperature reduction at 473 K is sufficient to reduce and activate these clusters. In addition, reduction of these clusters on carbon appears to be more facile and complete than on many oxide supports. In agreement with previous studies of bulk Fe–Ru alloys, surface enrichment in Fe seems to occur in these small crystallites after reduction although these particles do seem to retain an overall homogeneous composition, as expected from the bulk phase diagram. Methane and CO turnover frequencies increase in parallel with the increase in surface Ru concentration while the TOF for CO_2 formation smoothly decreases. The selectivity to CH_4, as represented by the ratio of CH_4 formation to total hydrocarbon formation, increases linearly with the overall Ru concentration, while the olefin/paraffin ratios remained low over all the catalysts prepared from Fe–Ru clus-

ters. The FeRu catalyst made by coimpregnation did not exhibit behavior consistent with that predicted by the mixed-metal cluster catalysts and indicates a lack of homogeneity in this catalyst. Initial STEM studies show that the metal crystallites are two-dimensional in nature and seem to form rafts within the small pores of the high-surface-area carbon used. This may be responsible for the stability of the kinetic behavior observed under reaction conditions. This investigation has shown that mixed-metal clusters can be used to produce active, bimetallic crystallites and that carbon is an excellent support to provide high dispersions and facilitate reduction of all the metal components.

ACKNOWLEDGMENTS

We are grateful to the National Science Foundation for support of this work through Grant CPE-8205937. We also acknowledge William Corbett for assistance in obtaining the STEM photographs.

REFERENCES

1. (a) Vannice, M. A., and Garten, R. L., paper 17, 67th AIChe Meeting, Washington, D.C., December 1974. (b) *J. Mol. Catal.* **1,** 201 (1975/76).
2. Vannice, M. A., Lam, Y., and Garten, R. L., "Hydrocarbon Synthesis," Adv. Chem Ser. 178, p. 26. Amer. Chem. Soc., Washington, D.C., 1979.
3. Ott, G. L., Fleisch, T., and Delgass, W. N., *J. Catal.* **60,** 394 (1979).
4. Sinfelt, J. H., "Advances in Catalysis," Vol. 23, p. 91. Academic Press, New York, 1973.
5. Anderson, J. R., and Mainwaring, D. E., *J. Catal.* **35,** 162 (1974).
6. Guczi, L., *Catal. Rev.-Sci. Eng.* **23,** 349 (1981).
7. Turney, T. W., Bruce, L., and Hope, G., *React. Kinet. Catal. Lett.* **20,** 175 (1980).
8. Anderson, J. R., Elmes, P. S., Howe, R. F., and Mainwaring, D. E., *J. Catal.* **50,** 508 (1977).
9. Robertson, J., and Webb, G., *Proc. R. Soc. London Ser. A* **341,** 383 (1974).
10. Guczi, L., Schay, Z., and Lazar, K., *Surf. Sci.* **106,** 516 (1981).
11. Jung, H. J., Walker, P. L., Jr., and Vannice, M. A., *J. Catal.* **75,** 416 (1982).
12. Vannice, M. A., and Garten, R. L., *J. Catal.* **63,** 255 (1980).
13. Aika, K., Hori, H., and Ozaki, A., *J. Catal.* **27,** 424 (1972).
14. McFarlane, W., and Wilkinson, G., *Inorg. Synth.* **8,** 181 (1969).
15. Eady, R. E., Jackson, P. F., Johnson, B. F. G., and Lewis, J., *J. Chem. Soc., Dalton Trans.*, 383 (1980).
16. Yawney, D. B. W., and Stone, F. G. A., *J. Chem. Soc. (A)*, 502 (1969).
17. Geoffroy, G. L., Fox, J. R., Burkhardt, E., Foley, H. C., Harley, A. D., and Rosen, R., *Inorg. Synth.* **21,** 58 (1982).
18. Shriver, D. F., "The Manipulation of Air-Sensitive Compounds." McGraw–Hill, New York, 1969.
19. Vannice, M. A., Walker, P. L., Jr., Jung, H.-J., Morena-Castilla, C., and Mahajan, O. P., "Proceedings, 7th International Congress on Catalysis, Tokyo, 1980." Paper A31, p. 460. Elsevier, Amsterdam, 1981.
20. Jung, H. J., Vannice, M. A., Mulay, L. N., Stanfield, R. M., and Delgass, W. N., *J. Catal.* **76,** 208 (1982).
21. Yoon, K. J., Walker, P. L., Jr., Mulay, L. N., and Vannice, M. A., *Ind. Eng. Chem. Prod. Res. Dev.* **22,** 519 (1983).
22. Topsøe, H., Topsøe, N., and Bohlbro, H., "Proceedings, 7th International Congress on Catalysis, Tokyo, 1980," p. 247. Elsevier, Amsterdam, 1981.
23. Dalla Betta, R. A., *J. Catal.* **34,** 57 (1974).
24. Boudart, M., Delbouille, A., Dumesic, J. A., Khammouma, S., and Topsøe, H., *J. Catal.* **37,** 486 (1975).
25. Kobayashi, M., and Shirasaki, T., *J. Catal.* **28,** 289 (1971).
26. Guerra, C. R., and Schulman, J. A., *Surf. Sci.* **7,** 229 (1967).
27. Yates, D. J. C., Murrell, L. L., and Prestridge, E. B., *J. Catal.* **57,** 41 (1979).
28. Bartholomew, C. H., and Pannell, R. B., *J. Catal.* **65,** 390 (1980).
29. Gay, I. D., *J. Catal.* **80,** 231 (1983).
30. Kellner, C. S., and Bell, A. T., *J. Catal.* **75,** 251 (1982).
31. Yang, C. H., and Goodwin, J. G., Jr., *React. Kinet. Catal. Lett.* **20,** 13 (1982).
32. Elliott, R. P., "Constitution of Binary Alloys," p. 431, 1st suppl. McGraw–Hill, New York, 1965.
33. Ott, G. L., Fleisch, T., and Delgass, W. N., *J. Catal.* **60,** 394 (1979).
34. Ott, G. L., Delgass, W. N., Winograd, N., and Baitinger, W. E., *J. Catal.* **56,** 174 (1979).
35. Schabes-Retchkiman, P., Gomez, A., Vazquez-Polo, G., and Jose-Yacaman, M., *J. Vac. Sci. Technol.* **A2(1),** 22 (1984).
36. Ott, G. L., Fleisch, T., and Delgass, W. N., *J. Catal.* **65,** 253 (1980).
37. McKee, D. W., *J. Catal.* **8,** 240 (1967).

38. Vannice, M. A., *J. Catal.* **37,** 449 (1975).
39. Guczi, L., Schay, Z., Matusek, K., Bogyay, I., and Steffler, G., *in* "Proceedings, 7th International Congress on Catalysis, Tokyo, 1980" (T. Seiyama and K. Tanabe, Eds.), p. 211. Elsevier, New York, 1981.
40. Dalla Betta, R. A., Piken, A. G., and Shelef, M., *J. Catal.* **35,** 54 (1974).
41. Dalla Betta, R. A., Piken, A. G., and Shelef, M., *J. Catal.* **40,** 173 (1975).
42. King, D. L., *J. Catal.* **51,** 386 (1978).
43. Garten, R. L., *J. Catal.* **43,** 18 (1976).
44. Ekerdt, J. G., and Bell, A. T., *J. Catal.* **58,** 170 (1979).
45. Kellner, C. S., and Bell, A. T., *J. Catal.* **70,** 418 (1981).